Journal of Fluids and Structures (1998) **12,** 759–777
Article No: fl980157

VORTEX-INDUCED OSCILLATION AND LIFT OF YAWED CIRCULAR CYLINDERS IN CROSS-FLOW

K. Nakagawa, K. Kishida and K. Igarashi

Faculty of Engineering, Osaka University
2-1 Yamadaoka, Suita, Osaka 565, Japan

(Received 17 January 1997 and in revised form 5 February 1998)

This paper presents the wind-tunnel test data for vortex-induced oscillations of yawed circular cylinders in cross-flow. The experiments were conducted on free oscillation models for yaw angles of $\theta = 0, 15, 30$ and 45°, and for different values of reduced damping or Scruton number. The structural damping was measured on each of the models. The test Reynolds number, in the subcritical region, ranged from 8×10^3 to 2×10^4. The amplitude of oscillation and the amplitude and phase angle of fluctuating lift were measured with respect to the reduced velocity. The flow velocity and force characteristics were computed by applying the "Cosine Law" for yawed cylinders. The data correlations for yawed cylinders based on the cosine law were in fair agreement with data previously presented for unyawed cylinders. The amplitude and phase angle of fluctuating lift in terms of the peak cylinder amplitude are shown. The lock-in region boundary of the reduced velocity and the peak cylinder amplitude in terms of the reduced damping are also given.

1. INTRODUCTION

VORTEX-INDUCED OSCILLATION of a circular cylinder in cross-flow, a problem in the general area of fluid – structure interaction phenomena, has received a great deal of attention both from the academic and practical points of view. For example, vibration problems have been experienced by many structures such as chimney stacks, towers, missiles, bridge decks, offshore structures, etc, which are exposed to wind or ocean currents. Many experimental and theoretical studies on the subject may be found in several excellent reviews; for example, Parkinson (1973), Sarpkaya (1979), Bearman (1984) and Parkinson (1989).

Hartlen & Curie (1970) proposed a mathematical model of the vortex-induced oscillation of a circular cylinder and derived a theory relating the cylinder displacement to the exciting lift force. Parkinson (1973), Sarpkaya (1978, 1979), Bearman (1984), Ericsson (1988), Parkinson (1989) and others also discussed mathematical models of the vortex-induced oscillation of a circular cylinder.

In a fluid flow in a certain Reynolds number range, vortices are shed alternately from either side of a circular cylinder. The resulting changes in circulation around the cylinder induce fluctuating fluid forces. If the frequency of the regular vortex shedding approaches the natural frequency of an elastic cylinder system, the amplitude of the cylinder vibrations can be amplified. The cylinder oscillation frequency f_c and the vortex-shedding frequency f_v could often lock-in to a common value close to the cylinder natural frequency f_n. It is generally accepted that the oscillation is of a self-excited nature in the lock-in range.

A number of measurements were made on unyawed and yawed circular cylinders in cross-flow in the subcritical range, using wind tunnels or water channels. A review of the very numerous unyawed cylinder experiments is presented first, followed by a review of yawed cylinder experiments.

0889-9746/98/060759 + 19 $30.00

The free-oscillation experiments of unyawed cylinders made by Scruton (1963) showed that the lock-in range of reduced velocity depends on the reduced damping. The free-oscillation tests conducted by Feng (1968) and Parkinson, Feng & Ferguson (1968) showed the relationship between the peak cylinder amplitude and the lock-in range of reduced velocity in terms of the reduced damping. The tests showed the existence of hysteresis behaviour. Data for the fluctuating lift force were also presented. The free-oscillation tests by Griffin & Koopman (1977) showed how the peak cylinder amplitude and the lock-in range depend on the reduced damping.

The forced-oscillation tests of unyawed cylinders conducted by Yano & Takahara (1971), Sarpkaya (1978) and Staubli (1983) demonstrated the response characteristics in terms of the magnitude and phase angle of the lift as a function of the cylinder oscillation amplitude. Nakamura, Kaku & Mizota (1971), Tanida, Okajima & Watanabe (1973) and Griffin & Koopman (1977) measured the lift component in phase with the cylinder velocity. Toebes (1969) showed the variation of the spanwise correlation of fluctuating velocities in the wake behind a circular cylinder with the amplitude of the cylinder oscillation. It can be seen from their results that the correlation length for a stationary cylinder is approximately one-third of the oscillating cylinder length. The correlation length increased drastically with cylinder amplitude in the lock-in region.

King (1977) conducted water channel experiments to study the vortex-excited oscillation of yawed circular cylinders at $\theta \leq 45^\circ$ in the subcritical range. An experimental justification of the cosine law was seen in his plots of A/d versus V_r, where $V_r = \mathrm{U}\cos\theta/f_n d$. Ramberg (1983) observed the vortex wakes behind stationary and oscillating yawed cylinders having large end-plates in the low Reynolds number range. It will be shown in this paper that the vortex-shedding frequencies were consistent with the cosine law.

This paper presents the wind-tunnel test data for vortex-induced oscillations of yawed circular cylinders in cross-flow. The experiments were conducted on spring-supported models for yaw angles of $\theta = 0, 15, 30$ and 45°, for different values of reduced damping. The structural damping of the models was measured with care. The Reynolds numbers ranged in the subcritical region from 8×10^3 to 2×10^4. The amplitude of cylinder oscillation and the lift coefficient and phase angle of fluctuating lift were measured. The flow velocity and force characteristics were computed by applying the cosine law. The results for the yawed cylinders based on the cosine law were compared and correlated with previous data on the unyawed circular cylinders presented by other researchers. The discussion is concentrated on verifying the validity of the cosine law for yawed oscillating cylinders.

2. THEORETICAL BASIS FOR YAWED CYLINDER VIBRATION

Consider a stationary cylinder yawed at an angle θ, where θ is the angle between the freestream direction and the axis normal to the cylinder. In this case, the flow and fluid force acting on the cylinder can be computed by a cross-flow velocity component normal to the cylinder axis $U\cos\theta$ as the characteristic velocity, instead of the freestream velocity U. The validity of this conjecture was verified experimentally by Jones (1947) by measuring the drag forces on circular cylinders at yaw angles ranging from $\theta = 0^\circ$ to $\theta = 90^\circ$. This was also demonstrated theoretically by Moore (1956). The application of a cross-flow velocity component has been called the "Cosine Law" or the "Independence Principle". Whenever the word "the Cosine Law" is used in the present paper, it implies a characteristic velocity defined by the cross-flow velocity component $U\cos\theta$, instead of the freestream velocity U.

The cosine law can also be expected to be valid for resolving the response characteristics of an oscillating cylinder. Consider free oscillation of a circular cylinder that is yawed to the

oncoming flow. The equation of motion for an elastically mounted, linearly damped and periodically forced cylinder may be written as

$$m\ddot{x} + c\dot{x} + kx = F(t), \tag{1}$$

where x is the transverse displacement of the cylinder, m the cylinder mass, c the structural damping coefficient, k the spring constant, $F(t)$ the forcing function of fluctuating lift, and the dot denotes the time derivative. The steady-state cylinder oscillation in the lock-in range may be considered to be harmonic, i.e.,

$$x = A\cos\omega_c t, \tag{2}$$

where A is amplitude of cylinder oscillation, and $\omega_c = 2\pi f_c$. By applying the cosine law to the fluctuating lift, the forcing function can be defined as

$$F(t) = \tfrac{1}{2}\, C_{L\theta}\rho U^2 \cos^2\theta L d\cos(\omega_c t + \phi), \tag{3a}$$

$$F(t) = \tfrac{1}{2}\, C_L \rho U^2 L d\cos(\omega_c t + \phi), \tag{3b}$$

where $C_{L\theta}$ is the lift coefficient computed by taking $U\cos\theta$ as the flow velocity. C_L being the lift coefficient computed by taking U as the flow velocity, ρ is the fluid density, L the cylinder length immersed in the flow, d the cylinder diameter, and ϕ the phase angle. From equations (3a) and (3b), we get the relation

$$C_L = C_{L\theta}\cos^2\theta. \tag{4}$$

We next substitute equations (2) and (3a) into equation (1), which can then be rewritten as

$$\begin{aligned} m[\, &-\omega_c^2 A\cos\omega_c t - 2\zeta\omega_n\omega_c A\sin\omega_c t + \omega_n^2 A\cos\omega_c t] \\ &= \tfrac{1}{2}\, C_{L\theta}\rho U^2\cos^2\theta L d\cos(\omega_c t + \phi), \end{aligned} \tag{5}$$

where $\omega_n = \sqrt{k/m}$ is the natural radian frequency and $\zeta = c/2\sqrt{mk}$ is the structural damping ratio.

The method of Hartlen & Currie (1970) for unyawed cylinder analysis may be adapted and extended for flow over a yawed cylinder. Hence, the following relations may be derived by collecting the coefficients of $\cos\omega_c t$ and $\sin\omega_c t$ in equation (5), respectively,

$$2\pi^3\left[1 - \frac{f_c^2}{f_n^2}\right]\frac{\mu}{V_r^2}\,\frac{A}{d} = C_{L\theta}\cos\phi \tag{6}$$

and

$$4\pi^3\zeta\,\frac{f_c}{f_n}\,\frac{\mu}{V_r^2}\,\frac{A}{d} = C_{L\theta}\cos\phi, \tag{7}$$

where $\mu = m/[(\pi/4)\,(\rho L d^2)]$ is the mass ratio, and $V_r = \mathrm{U}\cos\theta/f_n d$ is the reduced velocity based on the cosine law. Equation (7) represents a balance between the structural damping and the lift component in phase with the cylinder velocity.

By introducing the structural logarithmic decrement $\delta_s = 2\pi\zeta$ and the reduced damping $\delta_r = 2m\delta_s/\rho L d^2$, equation (7) can be written as

$$4\pi\frac{f_c}{f_n}\,\frac{\delta_r}{V_r^2}\,\frac{A}{d} = C_{L\theta}\cos\phi. \tag{8}$$

Equation (8) shows that the reduced damping δ_r controls the amplitude of the oscillation in the lock-in range.

3. EXPERIMENTAL ARRANGEMENT AND PROCEDURE

3.1. Wind Tunnel And Measuring Technique

The experiments were conducted in a closed-circuit wind tunnel with a rounded-corner test-section having a cross-section of 1·2 m × 1·2 m and a length of 3·5 m. The maximum wind speed was approximately 50 m/s. The flow velocity was uniform within an accuracy of $\pm$ 0·87% and with a turbulence level less than 0·32%. The measurements were made on elastically mounted circular cylinders which were yawed in the flow. The time histories of the transverse cylinder oscillation and the fluctuating lift were measured at various wind velocities. The test wind velocities ranged from 2 to 4·5 m/s, and the corresponding subcritical range Reynolds numbers were from 8×10^3 to 2×10^4, based on the freestream velocity.

The experimental arrangement is shown in Figures 1 and 2. The dimensions of the cylinder models are listed in Table 1. The circular cylinders were 60 mm in diameter. Cylinders of two different lengths were used: $L = 1\,950$ mm for conducting the unyawed cylinder tests and yawed cylinder tests at $\theta = 0,\ 15$, and 30°; and $L = 2650$ mm for yawed cylinder tests at $\theta = 45^\circ$. Each cylinder model was installed in the tunnel by passing through slots of the tunnel walls, and was suspended horizontally by four coil-tension springs at both ends outside the test-section. In that state, the cylinder was free to oscillate vertically.

The end effects produced by tunnel-wall interference were minimized by installing end-plates to the cylinders at the tunnel sidewalls. Circular end-plates, 240 mm in diameter, were designed for tests with at $\theta = 0$, 15 and 30° and elliptical end-plates of 240 mm × 260 mm for the $\theta = 45^\circ$ tests. A 10 mm gap was set up between the plates and the walls. The spring constant was 21880 N/m for all the models tested.

The cylinder displacement was sensed by an eddy current displacement transducer outside the test section. The signals were displayed on an X–Y recorder.

Each cylinder was composed of three segments: two side-cylinders supporting a test segment of the force-measuring cylinder, as seen in Figure 2. The side-cylinders were constructed of aluminium alloy pipes. Two side-cylinders were rigidly joined by a connecting rod to create a single unit. The force-measuring cylinder made of a light acrylic-resin

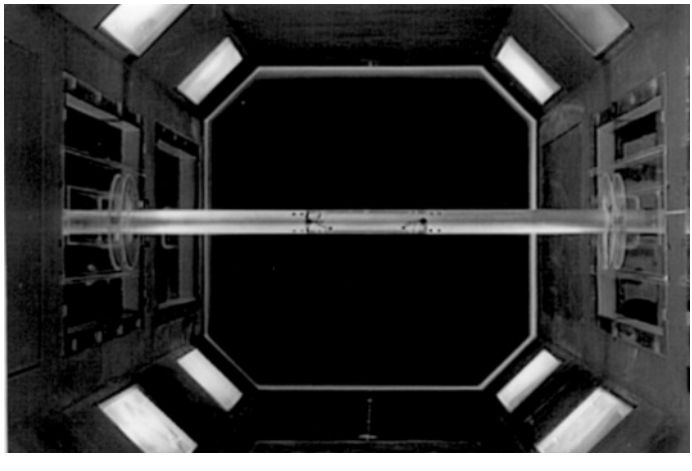

Figure 1. Photograph of the free-oscillation model.

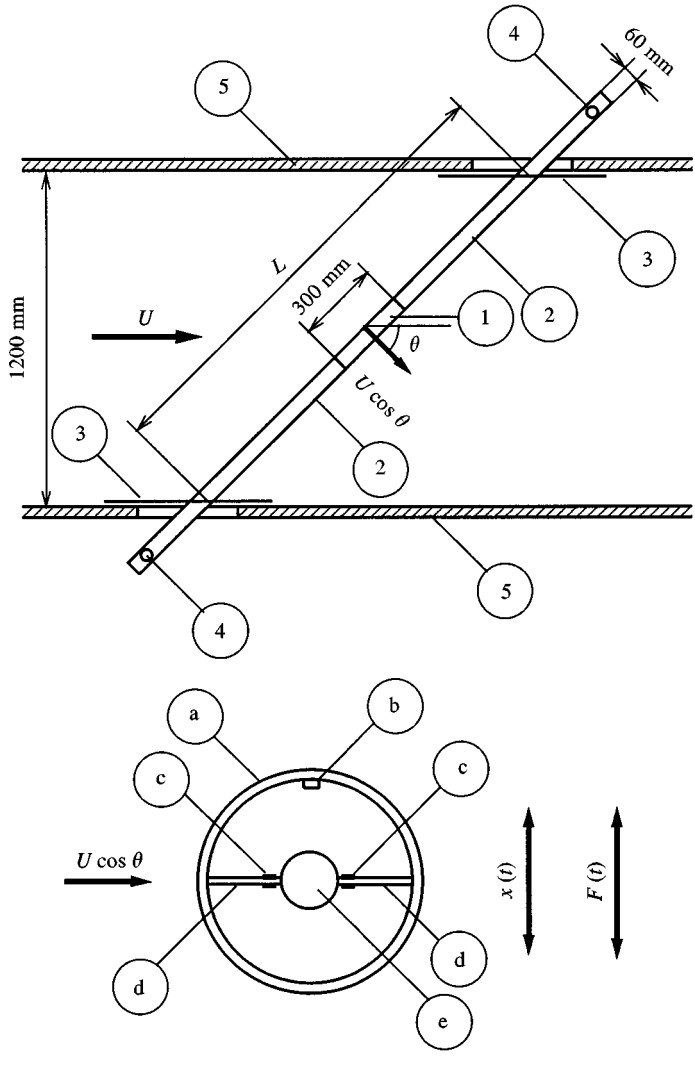

Figure 2. Instrumentation for test cylinders and force-measuring cylinder. ① force-measuring cylinder; ② side cylinder; ③ end-plate; ④ coil spring; ⑤ tunnel side wall; ⓐ force-measuring cylinder; ⓑ accelerometer, ⓒ strain gauges, ⓓ plate spring, ⓔ connecting rod.

pipe, 300 mm long, was installed on the connecting rod by four plate springs. Strain gauges were cemented on each plate spring to sense the applied force. The strain gauge signals were amplified by a Wheatstone bridge and the results were displayed on an X–Y recorder.

The equation of motion for the force-measuring cylinder can be obtained as

$$F_t(t) = m'\ddot{y} + c'(\dot{y} - \dot{x}) + k'(y - x), \tag{9}$$

where $F_t(t)$ is the force acting on the force-measuring cylinder, m′ the mass of the force-measuring cylinder, c' the damping coefficient, k' the spring constant, x the transverse displacement of the side-cylinders, and y the displacement of the force-measuring cylinder. In this test, the inertia force $m'\ddot{y}$ was estimated from the output of an accelerometer installed on the cylinder. The lift force signal was obtained by subtracting the inertia force signal

TABLE 1
Circular cylinder models

Yaw angle, θ (deg)	0		15		30		45	
Cylinder diameter, d (mm)	60		60		60		60	
Length immersed to flow, L (mm)	1220		1260		1400		1700	
Aspect ratio, L/d	20·3		21·0		23·3		28·3	
Cylinder mass, m (kg)	5·89	11·66	5·89	11·66	5·89	11·66	7·33	13·14
Mass per unit length, m/L (kg/m)	4·83	9·56	4·67	9·25	4·21	8·33	4·31	7·73
Natural frequency, f (Hz)	9·7	6·9	9·7	6·9	9·7	6·9	8·7	6·5
Log decrement in still air, (10^{-3})	2·32	1·83	2·07	2·06	2·00	1·98	1·95	1·86
Structural log decrement, (10^{-3})	1·70	1·70	1·70	1·70	1·70	1·70	1·70	1·70
Reduced damping, $2m\delta_s/Ld^2$	3·65	7·18	3·53	6·96	3·18	6·26	3·26	5·85

from the total force signal by using a subtracting circuit as

$$F(t) = c'(\dot{y} - \dot{x}) + k'(y - x). \tag{10}$$

The phase difference ϕ was determined from the cross-spectrum of the lift force and the cylinder displacement. Prior to each test, the force signals were calibrated by applying known fluctuating forces of different frequencies in still air. Thus, we obtained the values of C_L and ϕ in equation (3b). From equation (4), we obtained the value of $C_{L\theta} = C_L/\cos^2\theta$.

The velocity fluctuations in the wake were measured by hot-wire pickups which were aligned to the freestream flow and positioned at a horizontal distance of $1{\cdot}7d$ and a vertical distance of $1{\cdot}2d$ behind the cylinder centreline. The spanwise correlation and the spanwise phase difference in the wake behind the oscillating cylinders were measured by sweeping a movable hot wire along the cylinder spanwise separation distances.

The signals obtained in the tests were reduced and analyzed using a signal analyzer. The drag coefficient C_D and Strouhal number were measured on a stationary unyawed cylinder.

3.2. MODELS

The measurements were made on the circular cylinder models for yaw angles of $\theta = 0, 15, 30$ and 45°, for the different values of reduced damping of Scruton number, $\delta_r = 2m\delta_s/\rho Ld^2$, as listed in Table 1. Ideally, the structural damping δ_s should be determined from free vibration tests in vacuum. In the present paper, however, it was estimated from experiments in still air by the method proposed by Ogawa (1984). The total logarithmic decrement δ is determined by free vibrations of the damped system in stationary air, with different cylinder masses. Plots of $m\delta$ versus m fall on a single straight line: $m\delta_s + c$, where c is a constant resulting from the fluid damping. The value of δ_s can be accurately determined from this relation.

4. DISCUSSION OF EXPERIMENTAL RESULTS

4.1. DATA FOR A STATIONARY CIRCULAR CYLINDER

The drag coefficient $C_D = 1{\cdot}25$ for the stationary unyawed cylinder was measured at $\mathrm{Re} = 2\text{–}3 \times 10^4$. The measurements of vortex-shedding frequency yielded a Strouhal number $S = 0{\cdot}202$ at $\mathrm{Re} = 1{\cdot}45 \times 10^4$. Both of these values agree reasonably well with the previously reported ones.

4.2. Response Characteristics of Cylinders

The lock-in cylinder oscillation occurred over a limited range of wind velocities between 2 and 5 m/s. The corresponding Reynolds number was 8×10^3 to 2×10^4. For a given test-cylinder configuration, the experiment was started from the lowest wind velocity. The collection of data was started under steady-state conditions, after the starting transient oscillation was stabilized. Then, a stepwise increase in the velocity was made, by a set increment, and the next experiment started.

Figure 3 shows the typical response characteristics of an unyawed cylinder for a reduced damping $\delta_r = 3{\cdot}65$. The cylinder oscillation frequency f_c, the cylinder natural frequency f_n, and the vortex-shedding frequency f_v for a stationary cylinder are compared in the upper plot, and the normalized cylinder oscillation amplitude A/d in the lower plot. Both sets of data are plotted against a common wind velocity. As was expected, the observable oscillation started a wind speed where the vortex-shedding frequency f_v approached the natural frequency f_n. The peak amplitude was attained at a wind speed somewhat higher than for $f_n = f_v$. The cylinder oscillation frequency f_c was found to be very close f_n.

Figures 4–7 show the response characteristics of the unyawed and yawed cylinders for $\theta = 0, 15, 30$ and 45°, for several values of reduced damping , $\delta_r = 2m\delta_s/\rho L d^2$. The phase

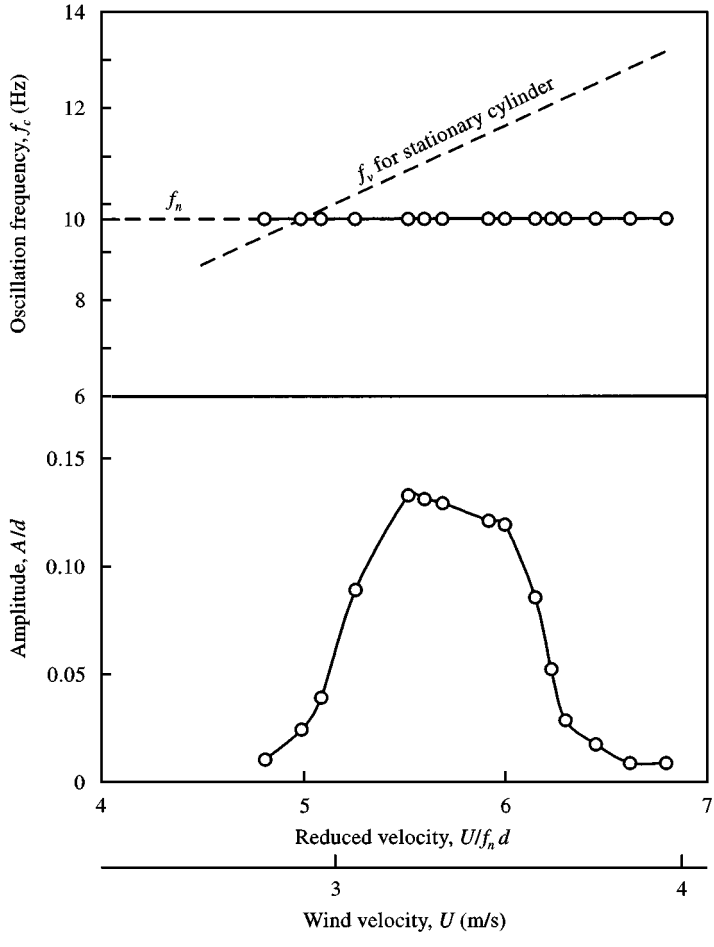

Figure 3. Response characteristics of an unyawed cylinder for $\delta_r = 3{\cdot}65$.

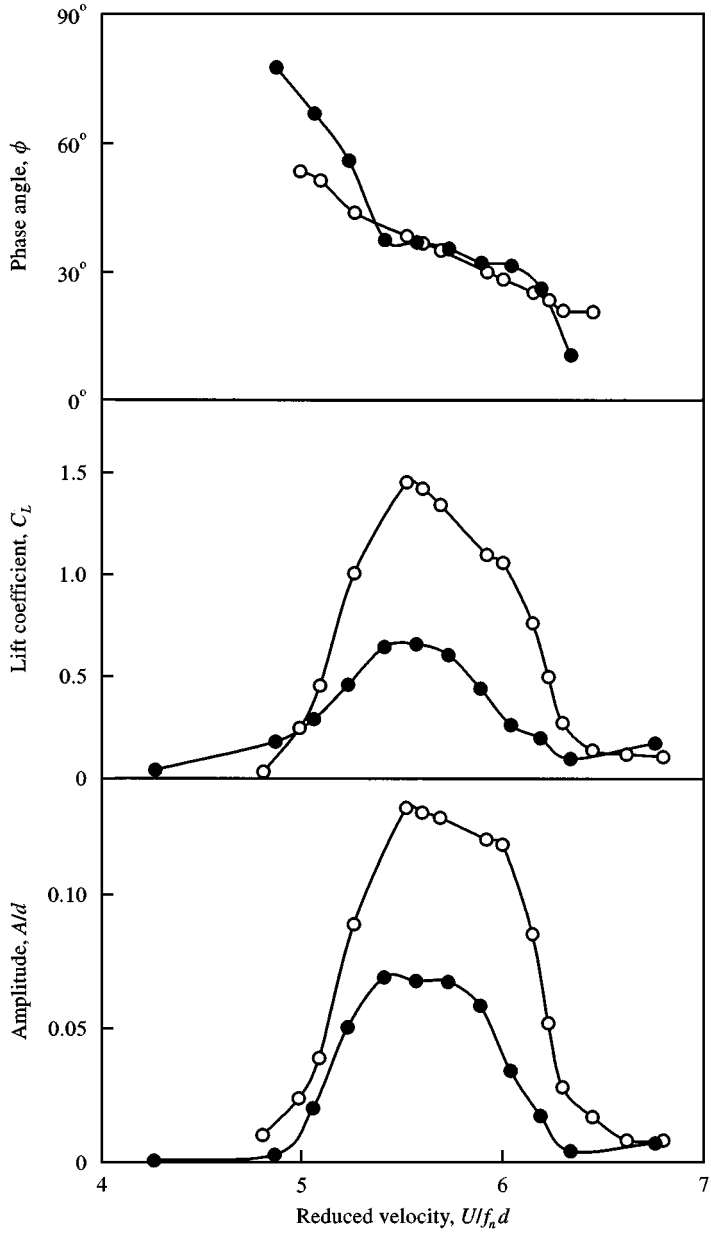

Figure 4. Response characteristics of unyawed cylinders: ○, $\delta_r = 3{\cdot}65$; ●, $\delta_r = 7{\cdot}18$.

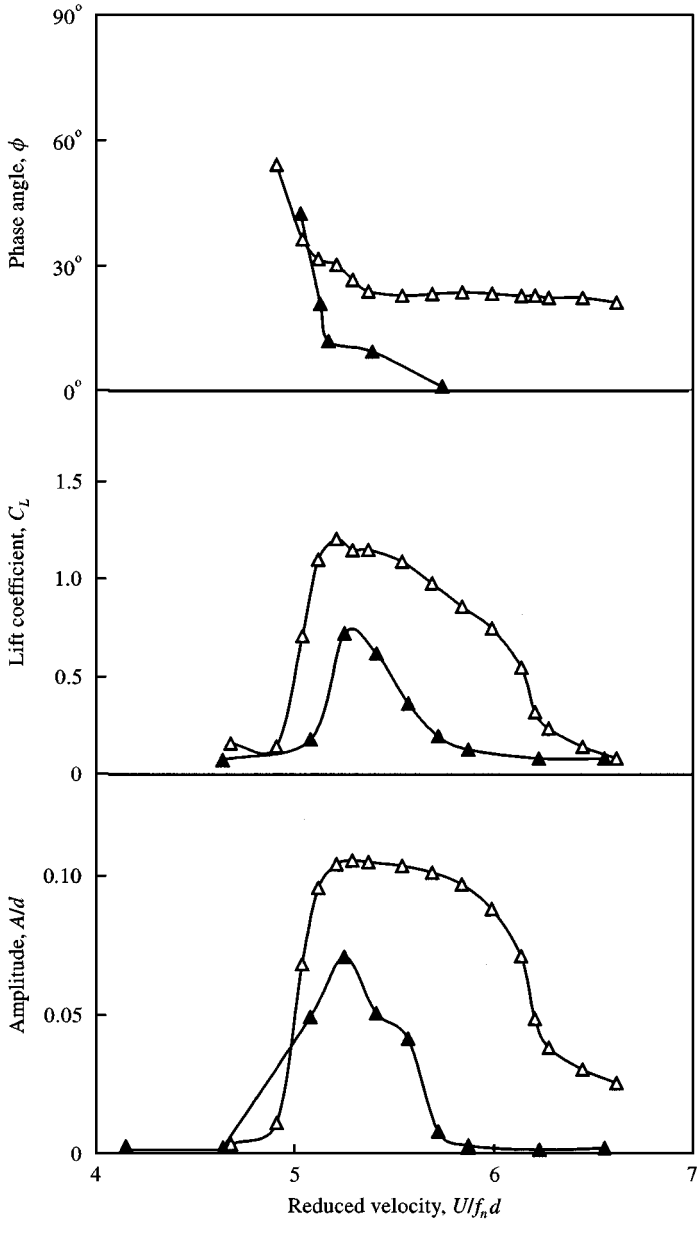

Figure 5. Response characteristics of a yawed cylinder for $\theta = 15°$: △, $\delta_r = 3{\cdot}53$; ▲, $\delta_r = 6{\cdot}96$.

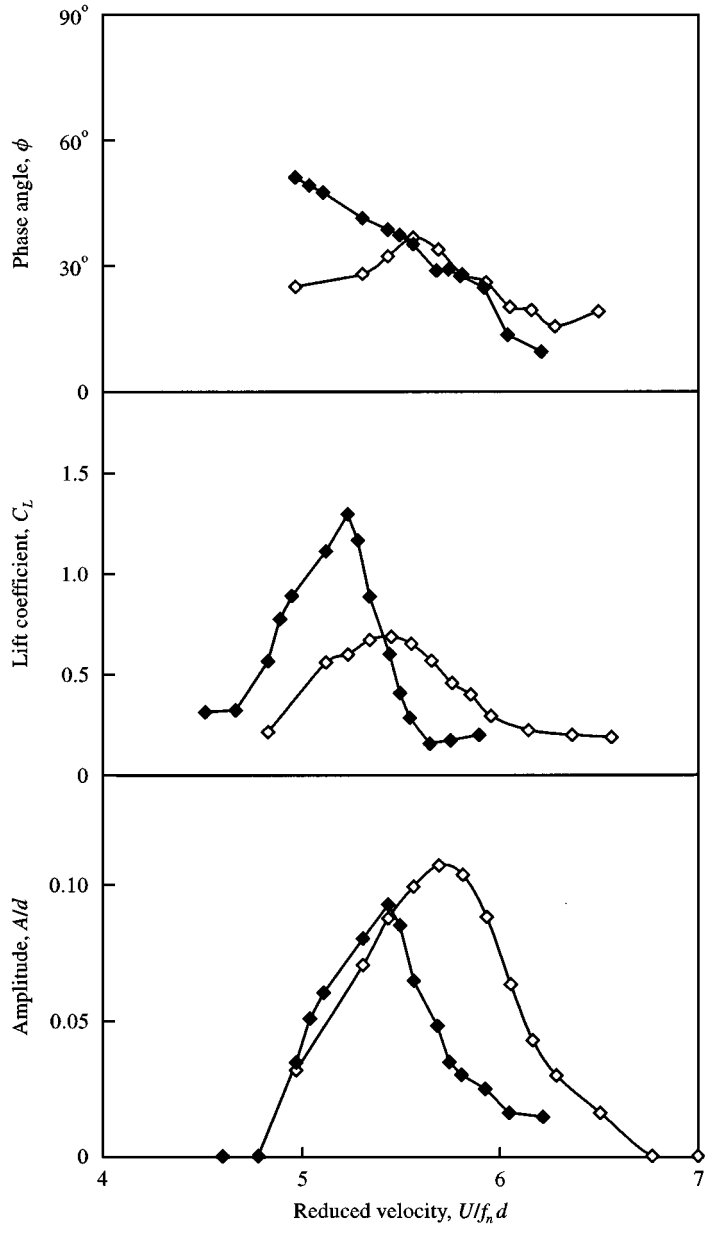

Figure 6. Response characteristics of a yawed cylinder for $\theta = 30°$: ◇, $\delta_r = 3{\cdot}18$; ◆, $\delta_r = 6{\cdot}26$.

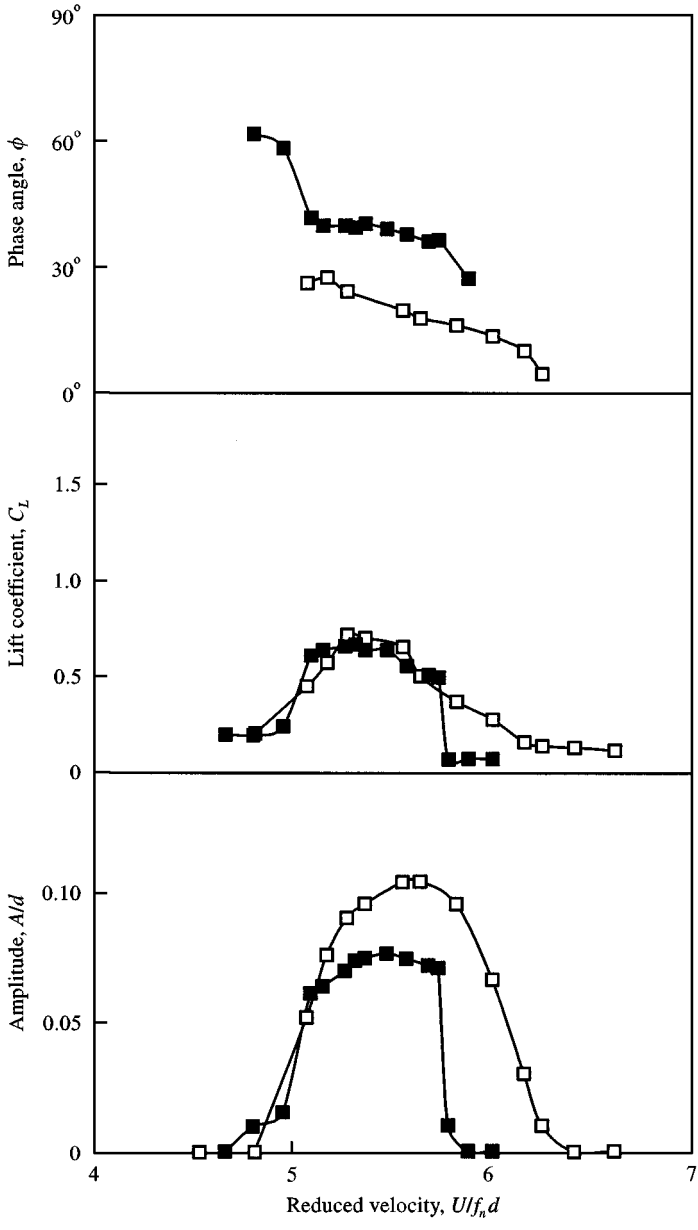

Figure 7. Response characteristics of a yawed cylinder $\theta = 45°$: □, $\delta_r = 3{\cdot}26$; ■, $\delta_r = 5{\cdot}85$.

angles ϕ, the lift coefficients C_L and the normalized amplitudes A/d are plotted against the reduced velocity V_r. It must be noted that $C_L = (\text{amplitude of } F)/(\frac{1}{2}\rho U^2 L d)$ and $V_r = U\cos\theta/f_n d$ have been computed by using the cosine law.

It is seen from these figures that the normalized peak amplitudes of the oscillating cylinders of the present tests were relatively low, approximately $0{\cdot}07 \leq A/d \leq 0{\cdot}13$. This is because the values of reduced damping, δ_r, of the present test configurations were rather high, because of heavier cylinder masses. However, a typical qualitative trend of decreasing peak amplitudes of lift and cylinder displacement with an increasing reduced damping was established and can be observed in these data plots.

It is well known that discontinuous change in the cylinder response at the peak amplitude was often observed in vortex-induced oscillations (see Parkinson 1989). However, it is noted that no discontinuous change appeared in the present data. It is speculated that a discontinuous change typically appears in high-amplitude oscillations but tends to disappear for low-amplitude oscillations, for example $A/d \simeq 0{\cdot}1$, for a cylinder with high damping. This phenomenon can also be observed in the experiments by Feng (1968), Feng & Ferguson (1968) Parkinson (1989) and Zdavkovich (1990).

4.3. Response Characteristics of Yawed and Unyawed Cylinders

Figure 8 compares the response characteristics of the yawed cylinder at $\theta = 45^\circ$, $\delta_r = 3{\cdot}65$ and the unyawed cylinder at $\theta = 0^\circ$, $\delta_r = 3{\cdot}26$. The figure suggests that the cosine law is valid for yaw angles at least up to $\theta = 45^\circ$. It is noted that a comparison of the response characteristics of a yawed cylinder computed by using the cosine law with that of the unyawed cylinder having the same reduced damping may be expected to satisfy the following characteristics: (i) the lock-in ranges of reduced velocity $U\cos\theta/f_n d$ are similar: (ii) the cylinder amplitude versus the reduced velocity are related by $(A/d)_\theta = (A/d)_{\theta=0}\cos\theta$: (iii) the phase angle ϕ versus the reduced velocity are similar, and (iv) the lift coefficient C_L versus the reduced velocity are related by $(C_L)_\theta = (C_L)_{\theta=0}\cos^2\theta$. Therefore, the response characteristics of a yawed cylinder may be estimated from the unyawed cylinder data for the same reduced damping.

Figure 9 shows the phase angle ϕ and the lift coefficient $C_{L\theta}$, which is based on the cosine law, against the peak amplitude of cylinder oscillations. The present data represent the yawed circular cylinder experiments. For a comparison, the unyawed circular cylinder data (ϕ, C_L) obtained by other researchers are superimposed on the figure. Some of these experiments were made with free-oscillation models and some were forced-oscillation experiments as noted in the figure. For the comparison of fluctuating lift force in different measurements, it is important to draw attention to the length of force measuring cylinder and the end conditions on the cylinder model. This is because differences in configuration may affect the accuracy of force measurements. The length of the force-measuring cylinder in experiments by other researchers were as follows: Feng (1968), $l/d = 9$; Yano & Takahara (1971), $l/d = 10$ and $6{\cdot}7$; Sarpkaya (1978), l/d was unspecified; Staubli (1983), $l/d = 13$. A comment on the cylinder length for the present force measurements is given in the Appendix.

The use of large end-plates attached to models is recommended [see Stansby (1974) and Ramberg (1983)]. Feng did not attach end-plates to his model, Yano & Takahara used circular plates of $2d$, Sarpkaya did not show any end-plates and Staubli attached circular plates of $10d$. As can be observed in Figure 9, the present data are in fair agreement with Staubli's data that were measured on a model having large end-plates.

Figure 10 shows the reduced velocity of the lock-in region that each cylinder oscillated with $A/d > 0{\cdot}01$ and the peak cylinder amplitude versus the reduced damping for

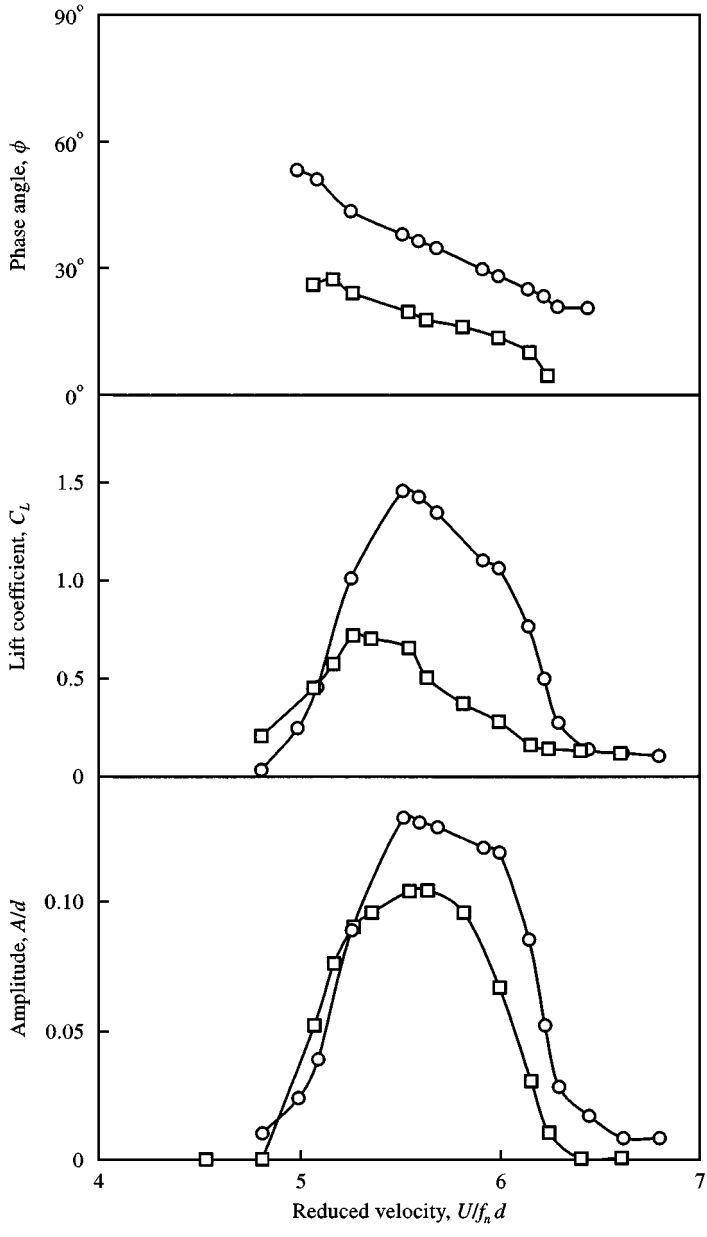

Figure 8. Comparison of response characteristics of unyawed with yawed cylinders: ○, $\theta = 0°$, $\delta_r = 3{\cdot}65$; □, $\theta = 45°$, $\delta_r = 3{\cdot}26$.

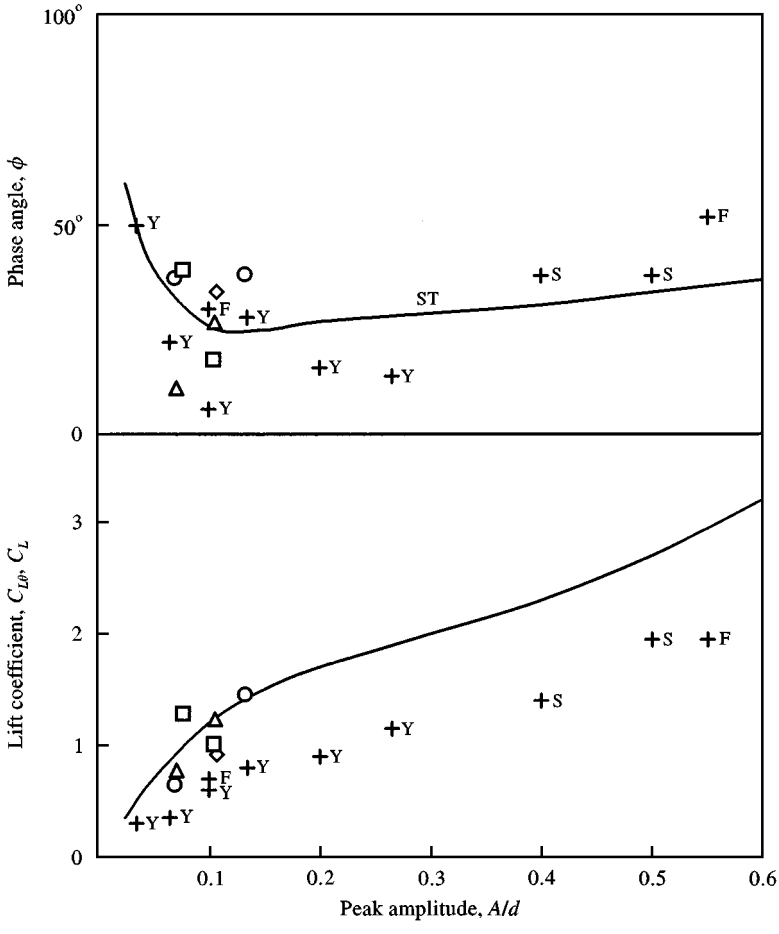

Figure 9. Lift coefficient and phase angle at peak oscillation amplitude. Present data †(C_{L0}, ϕ) : ○, $\theta = 0°$; △, $\theta = 15°$; ◇, $\theta = 30°$; □, $\theta = 45°$. Other data (C_L, ϕ) for unyawed cylinders: + F: Feng† (1968); + Y: Yano & Takahara§ (1971); + S: Sarpkaya† (1978); ST: Staubli§; (1983).

†: free oscillation model, §: forced-oscillation model.

the cylinders. The figure also includes the unyawed circular data obtained by other researchers.

Problems appear to have existed in estimating the value of structural damping $\delta_s = 2\pi\zeta$, used for computing the reduced damping $\delta_r = 2m\delta_s/\rho Ld^2$. As discussed in Section 3.2, the value of δ_s should be determined by a free oscillation test of the cylinder in the vacuum. Griffin & Koopman (1977) correctly measured the value by performing such experiments. However, the present authors estimated the value of δ_s using the data from the free oscillation of the cylinder in still air as described in Section 3.2. Feng (1968) obtained the value of δ_s for a streamlined bar having the same equivalent mass as the cylinder, by observing the decay of the oscillation in still air. King (1977) employed the value of the still-air decay of the cylinder oscillation to determine δ_s. Therefore, the magnitudes of δ_s may be larger than the real values by an unknown amount, due to fluid damping. Scruton (1963) estimated the value of ζ by applying equation (7) for the unyawed cylinder, using the

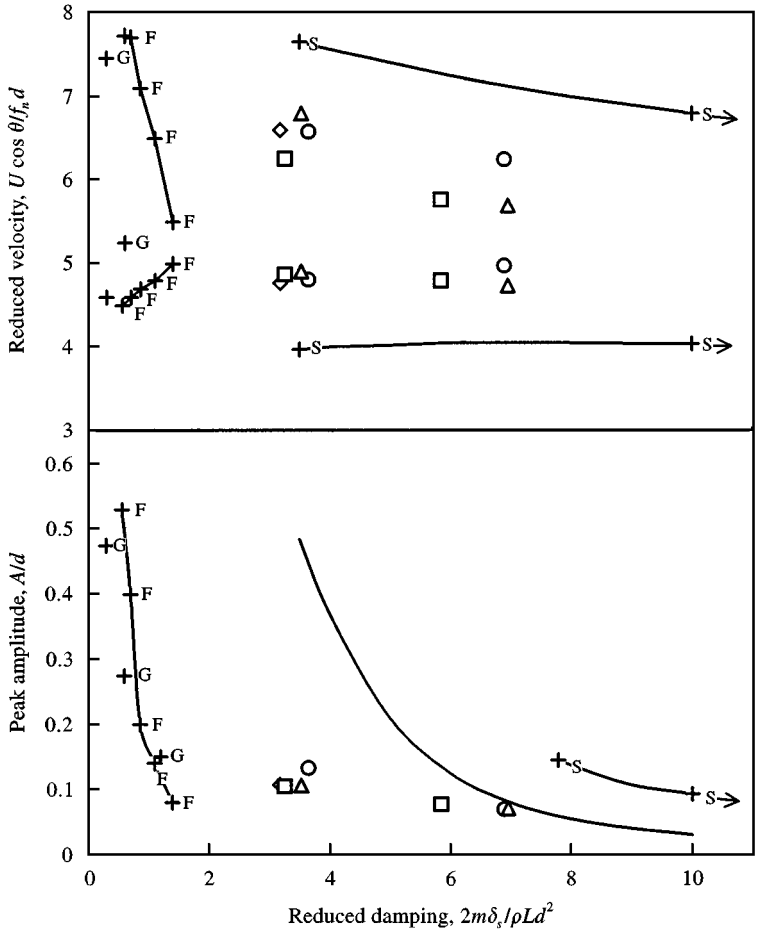

Figure 10. Lock-in region boundary and peak oscillation amplitude in terms of reduced damping. Present data: ○, $\theta = 0°$; △, $\theta = 15°$; $\theta = 30°$; □, $\theta = 45°$. Other data for unyawed cylinders ($\theta = 0°$): + S: Scruton (1963); + F: Feng (1968); + G: Griffin & Koopman (1977); K: King (1977).

measured lift forces which are in phase with cylinder velocity. The values obtained, however, often may be larger than the real ones, as pointed out by Parkinson (1973).

The data comparison of Figure 10 demonstrated that there is fair agreement between the present data and Griffin & Koopman's data, provided that their data can be asymptotically extrapolated into higher reduced damping.

It was observed in Figures 8–10 that the response characteristics of yawed cylinders may be estimated by applying the cosine law on the data presented for the unyawed cylinders. The response characteristics of the yawed cylinders followed the cosine law satisfactorily, at least up to $\theta = 45°$.

5. CONCLUSIONS

Free-oscillation experiments on circular cylinders at different yaw angles and different reduced damping were conducted in a closed-circuit wind tunnel. It was found that the response characteristics of the yawed cylinder followed the cosine law, at least up

to $\theta = 45^\circ$. These findings were substantiated by the present yawed circular cylinder data processed by the cosine law which were in fair agreement with the unyawed circular cylinder data presented by other researchers. The agreement was particularly good when the test cylinder configurations were matched, e.g. with respect to the aspect ratio of the force-measuring cylinder and whether end-plates were used, between the present test and the other ones.

It was also found that the normalized peak amplitudes of oscillation in the present tests were relatively low, i.e., approximately $0{\cdot}07 < A/d < 0{\cdot}13$. This is believed to be caused by the reduced damping in the present test configurations which were rather high because of the heavier cylinder masses involved. However, the typical qualitative trend of decreasing peak amplitudes of lift and displacement with increasing reduced damping was established in the present test.

ACKNOWLEDGEMENTS

The authors wish to express their gratitude to the late Prof. Yasuharu Nakamura, Associate Editor of the Journal of Fluids and Structures, for helpful discussions and suggestions. The authors wish to express cordial thanks to Dr Hideo Ikawa for valuable suggestions for the manuscript. Thanks also go to Dr M. Yamagiwa and Mr H. Ishihara for their assistance in conducting the experiments.

References

Bearman, P. W. 1984 Vortex shedding from oscillating bluff bodies. *Annual Reviews of Fluid Mechanics* **16,** 195–222.

Ericsson, L. E. 1988 Circular cylinder response to Karman vortex shedding. *Journal of Aircraft* **25**, 769–775.

Feng, C. C. 1968 The measurement of vortex induced effects in flow past stationary and oscillating circular and D-section cylinders. M. A. Sc. Thesis, University of British Columbia, Vancouver Canada.

Griffin, O. M. & Koopman, G. H. 1977 The vortex-excited life and reaction forces on resonantly vibrating cylinders. *Journal of Sound and Vibration* **54,** 435–448.

Hartlen, R. T. & Currie, I. G. 1970 Lift-oscillator model of vortex-induced vibration. *ASCE Journal of Engineering Mechanics* **96,** 577–591.

Jones, R. T. 1947 Effect of sweepback on boundary layer and separation. NACA Report **884**.

King, R 1977 Vortex excited oscillation of yawed circular cylinders. *ASME Journal of Fluids Engineering* **99,** 495–502.

Moore, F. K. 1956 Yawed infinite cylinders and related problems—Independence principle solutions. In *Advances in Applied Mechanics* (eds H. L. Dryden & Th. von Karman), Vol. 4, pp. 180–187. New York: Academic Press.

Nakamura, Y., Kaku, S. & Mizota, T. 1971 Effect of mass ratio on the vortex excitation of a circular cylinder. *Proceedings of Symposium on Buildings and Structures*, Tokyo, pp. 727–736.

Ogawa, K. 1984 An investigation of aerodynamic damping on airfoil and bluff body. *Proceedings of 8th National symposium on Wind Engineering*, Japan Association for Wind Engineering. Tokyo Paper 48 (in Japanese).

Parkinson, G. V. 1973 Mathematical models of flow-induced vibrations of bluff bodies. *In flow-induced Structural Vibration* (ed. E. Naudascher), pp. 81–127. Berlin: Springer.

Parkinson, G. V. 1989 Phenomena and modeling of flow-induced vibration of bluff bodies. *Progress of Aerospace Science* **26,** 169–224.

Parkinson, G. V., Feng, C. C., Ferguson, N. 1968 Mechanisms of vortex-excited oscillation of bluff cylinders. *Proceedings of Symposium on Wind Effects on Buildings and Structures*, Loughborough, . K., Paper 27.

Ramberg, S. E. 1983 The effects of yawed and finite length upon the vortex wakes of stationary and vibrating circular cylinders. *Journal of Fluid Mechanics* **128,** 81–107.

SARPKAYA, T. 1978 Fluid forces on oscillating cylinders. *ASCE Journal of Waterway Port Castral and Ocean Division* **104,** 275–290.
SARPKAYA, T. 1979 Vortex-induced oscillations—a selective review. *Journal of Applied Mechanics* **46,** 241–248.
SCRUTON, C. 1963 On the wind-excited oscillations of stacks, towers and masts. *Proceedings of Symposium on Wind Effects on Buildings and Structures*, N. P. L., U. K., pp. 798–821.
STANSBY, P. K. 1974 The effect of end plates on the base pressure coefficient of a circular cylinder. *Aeronautical Journal* **87,** 36–37.
STAUBLI, T. 1983 Calculation of the vibration of an elastically mounted cylinder using experimental data from forced oscillation. *ASME Journal of Fluids Engineering* **105,** 225–229.
TANIDA, Y. OKAJIMA, A. & WATANABE, Y. 1973 Stability of a circular cylinder oscillating in uniform flow or in a wake. *Journal of Fluid Mechanics* **61,** 768–784.
TOEBES, G. H. 1969 The unsteady flow and wake near an oscillating cylinder. *ASME Journal of Basic Engineering* **91,** 493–505.
YANO, T. & TAKAHARA, S. 1971 Study on unsteady aerodynamic force acting on an oscillating cylinder. *Proceedings of Symposium on Wind Effect on Buildings and Structures*, Tokyo, pp. 736–746.
ZDRAVKOVICH, M. M. 1990 On the origins of hysteretic responses of a circular cylinder induced by vortex shedding. *Zeitschrift für Flugwissenschaft und Weltraumforschung* **14,** 47–58.

APPENDIX A: COMMENT ON THE CYLINDER LENGTH FOR FORCE MEASUREMENTS

A comment will be given with respect to the influence on force measurements of the aspect ratio l/d of the force-measuring cylinder. It has been reported that accurate fluctuating lift measurements may be obtained by a short aspect ratio cylinder. The spanwise characteristic of wake flow behind an oscillating cylinder are dictated by the cylinder aspect ratio. Test data of spanwise correlation coefficients and spanwise phase difference of the wake flow velocity as functions of spanwise spacing are presented in Figures A.1 and A.2, respectively, for three amplitudes: $A/d = 0$ (stationary cylinder), 0·089 and 0·216.

For the present set-up, the cylinder aspect ratio of $l/d = 5$ was chosen as a reasonable value for a practical design. Therefore, the spanwise characteristics of wake flow may be estimated by taking the halfspan at $l/d = 2{\cdot}5$. Recall that the peak values of cylinder amplitudes A/d were measured as 0·07

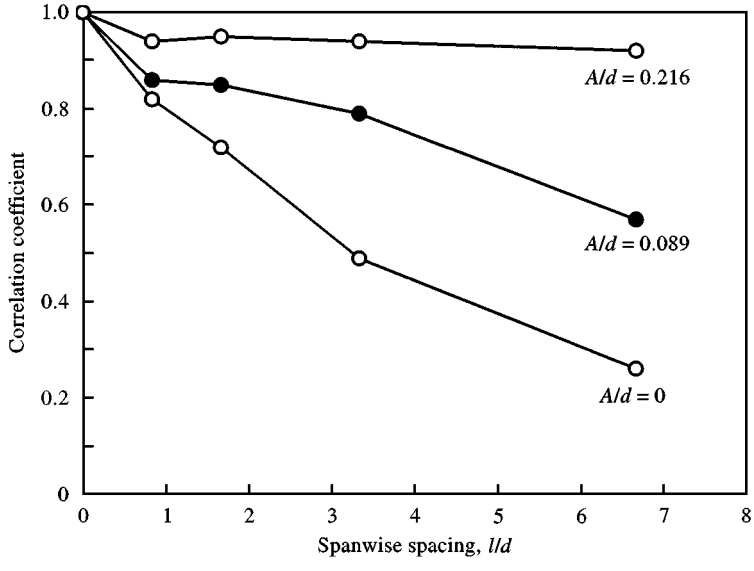

Figure A.1. Spanwise correlation of wake flow velocity of an unyawed cylinder: ○, $V_r = 5{\cdot}8$; ●, $V_r = 5{\cdot}4$.

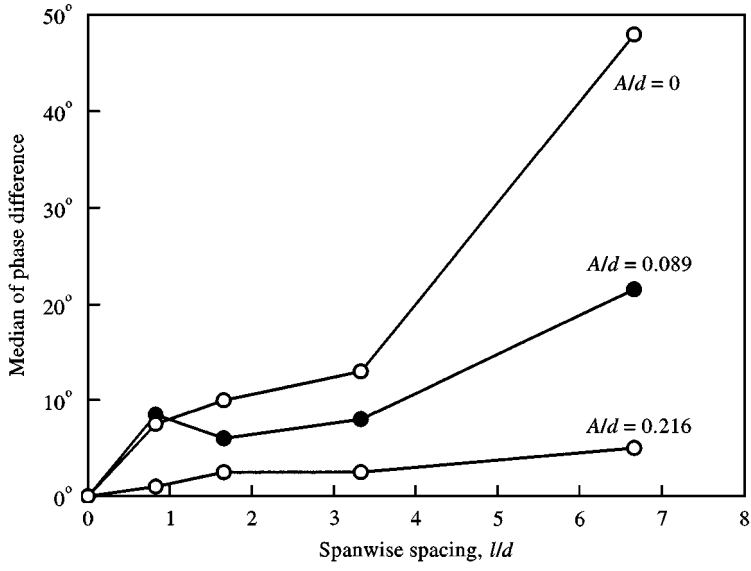

Figure A.2. Spanwise phase difference of wake flow velocity of an unyawed cylinder: ○, $V_r = 5{\cdot}8$; ●, $V_r = 5{\cdot}4$.

and 0·13 in the present test (Figure 4). At $l/d = 2{\cdot}5$, the spanwise correlation coefficients of wake flow velocity can be estimated as 0·75 to 0·85 for $A/d = 0{\cdot}07$ to 0·13, respectively (Figure A.1), and the spanwise phase differences of wake flow velocity are 9 to 5° for $A/d = 0{\cdot}07$ to 0·13, respectively (Figure A.2).

In view of the data obtained in this study the measurement accuracy of the lift coefficients $C_{L\theta}$ and phase angle ϕ (shown in Figure 9) can be estimated. The lift force can be computed by taking the mean of incident and wake flow velocities, as the characteristic flow velocity $U\cos\theta$. By applying the correlation data, the estimated $U\cos\theta$ deviations are ± 13 to $\pm 8\%$ for $A/d = 0{\cdot}07$ to 0·13, respectively. Because $C_{L\theta}$ is proportional to $1/(U\cos\theta)^2$, the estimated $C_{L\theta}$ deviations are $+31\%$ and -22 to $+18\%$ and -15% for $A/d = 0{\cdot}07$ to 0·13, respectively. Similarly, the estimated ϕ deviations are ± 5 to $\pm 3°$ for $A/d = 0{\cdot}07$ to 0·13, respectively.

For the measurements of fluctuating lift acting on a stationary circular cylinder, a very short length, say, $l/d = 0{\cdot}5$ to 1, has been recommended. By taking the halfspan at $l/d = 0{\cdot}5$, a spanwise correlation coefficient of wake flow velocity of 0·9 is obtained (Figure A.1). Also, the spanwise phase difference of wake flow velocity is 4° (Figure A.2). From these data, the estimated C_L deviation is $+11\%$ and -9% and the estimated ϕ deviation is $\pm 2°$. It is noted that exact force measurements can be achieved by fully instrumenting the cylinder periphery around a cross-section with pressure taps, as shown by Feng (1968).

APPENDIX B: NOMENCLATURE

A	amplitude
C_D	drag coefficient
C_L	lift coefficient
d	cylinder diameter
f_c	cylinder oscillation frequency
f_n	cylinder natural frequency
f_v	vortex shedding frequency
L	length of cylinder immersed to flow
l	length of force-measuring cylinder
m	cylinder mass
$\mathrm{R_e}$	Reynolds number
S	Strouhal number

U	freestream velocity
V_r	reduced velocity
x	transverse cylinder displacement
δ_s	structural damping
δ_r	reduced damping, $2m\delta_s/\rho Ld^2$
δ	total damping
ζ	structural damping ratio
θ	yaw angle
μ	mass ratio, $m/[(\pi/4)\ (\rho Ld^2)]$
ρ	fluid density
ϕ	phase angle
ω_n	natural radian frequency